Casing Convective Heat Transfer Coefficient and Reference Freestream Temperature Determination Near an Axial Flow Turbine Rotor

C. Camci
Professor
ASME Fellow

B. Gumusel
Graduate Research Assistant

Department of Aerospace Engineering,
Turbomachinery Aero-Heat Transfer Laboratory,
Pennsylvania State University,
223 Hammond Building,
University Park, PA 16802

The present study explains a steady-state method of measuring convective heat transfer coefficient on the casing of an axial flow turbine. The goal is to develop an accurate steady-state heat transfer method for the comparison of various casing surface and tip designs used for turbine performance improvements. The freestream reference temperature, especially in the tip gap region of the casing, varies monotonically from the rotor inlet to rotor exit due to work extraction in the stage. In a heat transfer problem of this nature, the definition of the freestream temperature is not as straightforward as constant freestream temperature type problems. The accurate determination of the convective heat transfer coefficient depends on the magnitude of the local freestream reference temperature varying in axial direction, from the rotor inlet to exit. The current study explains a strategy for the simultaneous determination of the steady-state heat transfer coefficient and freestream reference temperature on the smooth casing of a single stage rotating turbine facility. The heat transfer approach is also applicable to casing surfaces that have surface treatments for tip leakage control. The overall uncertainty of the method developed is between 5% and 8% of the convective heat transfer coefficient.
[DOI: 10.1115/1.4003757]

1 Introduction

Convective heat transfer to the static casing of a shroudless HP turbine rotor is a complex aerothermal problem. The unsteady flow with a relatively high Reynolds number in the tip gap region has strong dependency on the tip clearance gap, blade tip profile, tip loading conditions, tip geometry, and casing surface character. Thermal transport by flow near the casing inner surface is influenced by the unsteadiness, the surface roughness character, and the turbulent flow characteristics of the fluid entering into the region between the tip and casing. Since the turbine inlet temperatures are continuously elevated to higher levels, casing and tip related heat transfer issues are becoming more critical in design studies.

In gas turbines, the gas stream leaving the combustor is not at a uniform temperature in radial and circumferential directions. According to Butler et al. [1], the combustor exit maximum temperature can be twice as high as the minimum temperature. The maximum temperature in general is around the midspan and the lowest gas temperatures are near the walls. The mechanisms related to the distortion of the radial temperature profile as the combustor exit fluid passes through a turbine rotor are complex, as explained by Sharma and Stetson [2] and Harvey [3]. The hottest part of the fluid leaving the upstream nozzle guide vane tends to migrate to the rotor tip corner near the midpressure surface of the blade. Unfortunately, mostly the hottest fluid originating from the midspan region of the combustor or NGV finds its way to the pressure side corner of the blade tip in the rotating frame. Details of hot streak migration in gas turbines can be found in Refs. [4–8].

Contributed by the Heat Transfer Division of ASME for publication in the JOURNAL OF HEAT TRANSFER. Manuscript received May 3, 2010; final manuscript received December 13, 2010; published online xxxxx-xxxxx-xxxxx. Assoc. Editor: Frank Cunha.

Due to significant energy extraction in a HP turbine stage, the rotor absolute total temperature monotonically decreases in axial direction at a significant rate. This is especially true at the core of the blade passage where most of the energy extraction takes place. However, the fluid finding its way to the area between the casing and blade tips do not participate in the work generation as much as the midspan fluid. Therefore, it is reasonable to accept that the near-casing fluid does not cool as much as the midspan fluid when it progresses from rotor inlet to exit.

Yoshino [9] and Thorpe et al. [10] showed that a rotor blade can also perform work on the fluid near the casing surface by means of "rotor compressive heating." They obtained time-accurate and phase-locked casing heat flux measurements in Oxford Rotor Facility to show the casing heat loads as the rotor blades move relative to the static casing. They observed a very high heat flux zone on the casing inner surface for each blade in the rotor. Phase-locked measurements clearly indicated that the hot spot moved along the casing with the rotor. The results of this study showed two distinct levels of casing heating, one level for the casing interaction with the tip leakage fluid and a relatively low level for the casing interaction with the passage fluid located between blade tips. Thorpe et al. [10] explained the high heat flux zone on the casing surface by a rotor compressive heating model. They showed that the static pressure field near the tip can do work on the leakage fluid trapped between the blade tip and the casing. The rotor compressive heating model predicts that the absolute total temperature of the leakage fluid may exceed that of the rotor inlet flow. The flow near the casing turns and accelerates the leakage fluid to a tangential velocity level that is measurably above the rotor inlet level. Thorpe et al. [11] were successful in predicting the total temperature penalty due to compressive heating using the Euler work equation. Any design effort that will reduce the tip leakage mass flow rate in an axial turbine will also result in the reduction of the total temperature penalty and a corresponding reduction in casing heat load.

Past studies show three significant contributors to casing heat loads in shroudless HP turbines.

1. Radially outward and axial migration of a hot streak in each passage results in the accumulation of relatively high temperature fluid near the pressure side corner of the blade tip before it enters the tip gap.
2. A relatively higher total temperature in the near-casing fluid is observed because the near-casing fluid does not participate in stage work generation. The leakage fluid does not expand as much as the core-flow in the rotor passage.
3. Rotor compressive heating performed by blade tips when they move against the static casing is significant.

The near-casing gas temperature drops at a significant rate in axial direction. There is also a strong circumferential mixing near the casing because of the relative motion of blade tips. The time-accurate wall heat flux measured on the casing varies between a "passage gas induced low value" and "tip leakage fluid induced high value." Since near-casing gas temperatures vary at a significant rate in axial direction, any heat transfer measurement approach requires the simultaneous measurement of this local gas temperature in the vicinity of the casing, in addition to an accurate determination of convective heat transfer coefficient.

A steady state casing heat/mass transfer coefficient measurement method based on a naphthalene sublimation technique is explained in Ref. [12]. They reported similar casing heat transfer distributions with and without blade rotation. Their sublimation based heat transfer method is inherently intrusive because of the variations of the naphthalene layer thickness imposed by local mass transfer rate variations in the tip gap region.

The really difficult issues in casing heat transfer prediction are associated with gas path temperature redistribution and film cooling designs frequently applied in the casing region. Although a full simulation of gas temperature and casing cooling configurations is not attempted in the current study, a fundamental approach is followed for the accurate quantification of the fluid mechanics response of the viscous layers near the casing surface. Film cooling issues near the casing can be associated (a) with cooling bleed flow between the upstream vane platform and the casing leading edge, (b) with film cooling air originating from the blade pressure surface or from blade tip flows, or (c) from film cooling flowing through the casing itself. Items (a) and (b) could easily be explored using the test apparatus described in this paper if the rig were modified to include film cooling.

The present paper explains a steady-state method for the simultaneous determination of the casing heat transfer coefficient and the freestream reference temperature using a smooth casing in a single stage rotating turbine facility. The heat transfer approach is also applicable to casing surfaces with special surface treatments implemented for tip vortex desensitization. An uncertainty analysis follows a detailed description of the casing heat transfer measurements performed on a smooth casing surface.

2 Experimental Setup & Operation

Turbine Research Facility. The facility used for the current casing heat transfer study, shown in Fig. 1, is the Axial Flow Turbine Research Facility (AFTRF), at the Pennsylvania State University. A detailed description of the operational characteristics of this rotating rig is available in Ref. [13]. The research facility is a large-scale, low speed, cold flow turbine stage depicting many characteristics of modern high-pressure turbine stages. The total pressure and total temperature ratios across the stage are presented in Table 1 and air flow through the facility is generated by a four stage axial fan located downstream of the turbine. The rotor hub extends 1.7 blade tip axial chord length beyond the rotor exit plane. The turbine rig has a precision machined removable casing segment for measurement convenience especially for casing related aerothermal studies.

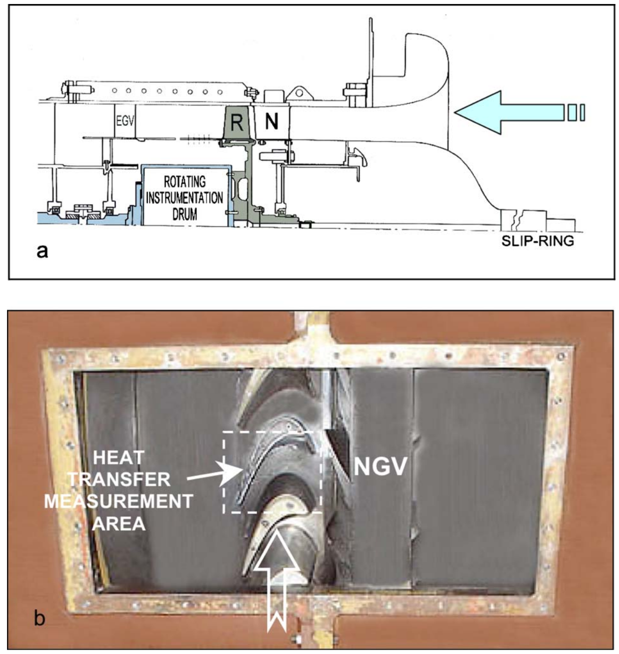

Fig. 1 AFTRF: (*a*) facility schematic and (*b*) window for the removable casing segment

A few of the relevant design performance data are listed in Table 1, while Table 2 lists important blade design parameters, including reaction at blade hub and tip sections, Reynolds number at rotor exit, and a few blade parameters. Measured/design values of rotor inlet flow conditions including radial, axial, and tangential components and data acquisition details of the turbine rig are explained in detail by Camci [13] and Rao et al. [14].

Instrumentation. Instruments used for monitoring the performance parameters of AFTRF consist of total pressure probes, Kiel probes, pitot-static probes, thermocouples, and a precision in-line torquemeter. The turbine rotational speed is kept constant around 1300 rpm by means of an eddy current brake.

Removable turbine casing. Figure 1(*b*) shows the facility removable casing segment as a convenient feature of the test facil-

Table 1 AFTRF facility design performance data

Inlet total temperature: T_{o1} (K)	289
Inlet total pressure: P_{o1} (kPa)	101.36
Mass flow rate: Q (kg/s)	11.05
Rotational speed: N (rpm)	1300
Total pressure ratio: P_{o1}/P_{o3}	1.077
Total temperature ratio: T_{o3}/T_{o1}	0.981
Pressure drop: $P_{o1}-P_{o3}$ (mm Hg)	56.04
Power: P (kW)	60.6

Table 2 AFTRF stage blade and vane data

Rotor hub-tip ratio	0.7269
Blade tip radius, R_{tip} (m)	0.4582
Blade height, h (m)	0.1229
Relative Mach number	0.24
Number of blades	29
Axial tip chord (m)	0.085
Spacing (m)	0.1028
Turning angle, tip/hub (deg)	95.42/125.69
Nominal tip clearance (mm)	0.9
Reaction, hub/tip	0.197/0.519
Reynolds number (-10^5) inlet/exit	(2.5–4.5)/(5–7)

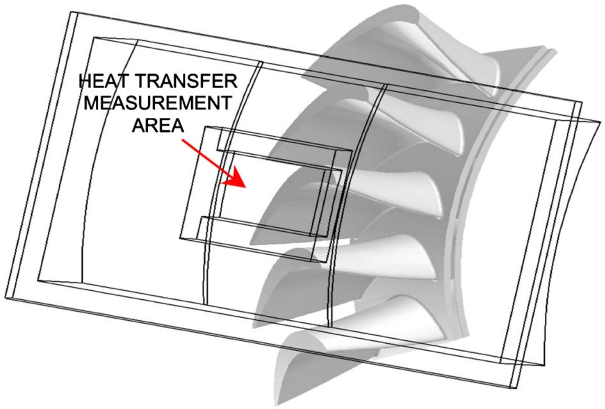

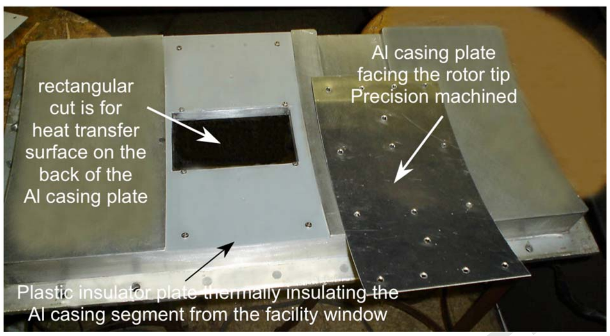

Fig. 2 Removable turbine casing in (AFTRF) (smooth partial "Al casing plate" is visible)

ity. A rectangular window is used to house the removable casing segment. This segment is a precision machined area designed for many different aerothermal measurement techniques to be applied around the turbine stage. Tip clearance is measured via a set of precision shim gages between the AFTRF casing and individual blade tip surfaces. The position of the aluminum plate with respect to the AFTRF casing is also accurately determined.

Figure 2 shows the removable segment with the rectangular central area (dashed boundaries Fig. 1(*b*)) allowing the researchers to perform casing heat transfer measurements. The "smooth" aluminum casing plate that is facing the rotor tip and interacting with near-casing fluid is also shown in Figs. 2 and 3. The Al casing plate could easily be replaced with custom made plates having special casing treatments for tip vortex aerodynamic desensitization and supporting heat transfer studies. The removable turbine casing and the Al plate are carefully designed and precision machined so that many subsequent installations of the same

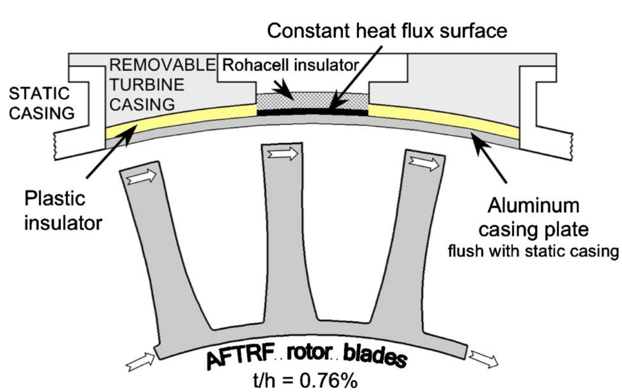

Fig. 3 Removable turbine casing cross section (normal to the axis of rotation)

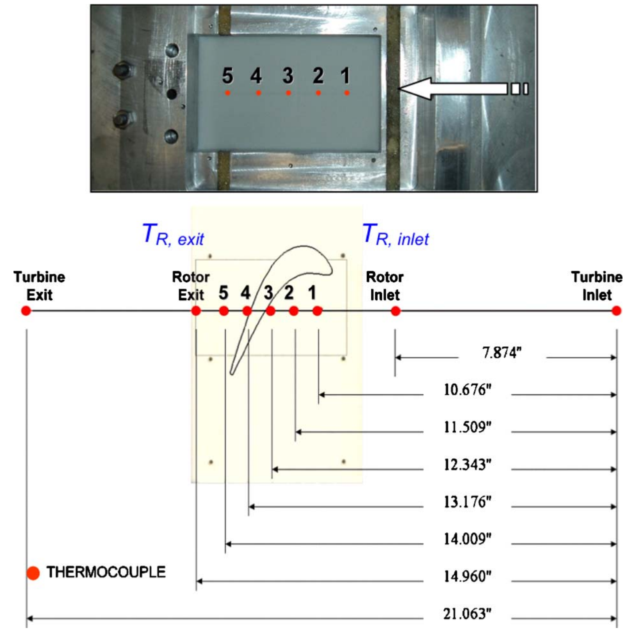

Fig. 4 Heat transfer coefficient measurement locations on the casing surface (five axial locations)

Al plate and the removable window/casing result in a repeatable tip clearance. Tip clearance repeatability within ± 25 μm (± 0.001 in.) for a blade height of 125 mm (4.85 in.) is possible. This uncertainty corresponds to a change in nondimensional tip clearance of $\pm 0.02\%$ of the blade height. Under normal circumstances, the inserted Al plate is supposed to be flush with the static casing of the facility. Slight clearance adjustments are possible for the removable segment by altering the thickness of the "plastic insulator," as shown in Fig. 3. The baseline Al casing plate has consistent radius of curvature with the casing. The average turbine tip clearance for the current experiments is kept at $t/h = 0.76\%$.

Heat transfer coefficient measurement locations. The five convective heat transfer coefficient measurement locations are shown in Fig. 4. Location 1 is closest to the leading edge of the blade in axial direction. The five selected measurement locations cover the axial distance between the blade leading edge and slightly downstream of the trailing edge. Due to the rotation of the blade, the steady-state heat transfer coefficient distribution in circumferential direction is reasonably uniform. Since work is extracted in the rotor, the freestream total temperature between the rotor inlet and rotor exit are different. Freestream total temperature measurement locations at the turbine inlet, rotor inlet, rotor exit, and turbine exit are also shown in Fig. 4. The freestream total temperatures at turbine inlet and exit are measured using calibrated K type thermocouples in a Kiel probe arrangement. Rotor inlet and exit thermocouples are inserted into the flow at about 25 mm away from the casing surface.

Steady-state heat transfer method. Casing convective heat transfer coefficients and corresponding freestream reference temperatures are measured simultaneously with the help of an embedded constant heat flux heater, as shown in Fig. 5. A constant heat flux heater (MINCO HK5175R176L12B) with an effective area of $A = 76 \times 127$ mm^2 is sandwiched between two thin Mylar sheets. The heater can produce a maximum of 75 W with an overall resistance of 176 Ω. The overall resistance of the 0.5 mm thick heater has extremely small temperature dependency in the range of the current experiments. This resistance value is continuously measured and recorded during each measurement. The Joule heating value in the heater is I^2R/A in W/m^2. The heat transfer surface has many flat ribbon thermocouples of type K imbedded at many locations (symbol ◙ in Fig. 5).

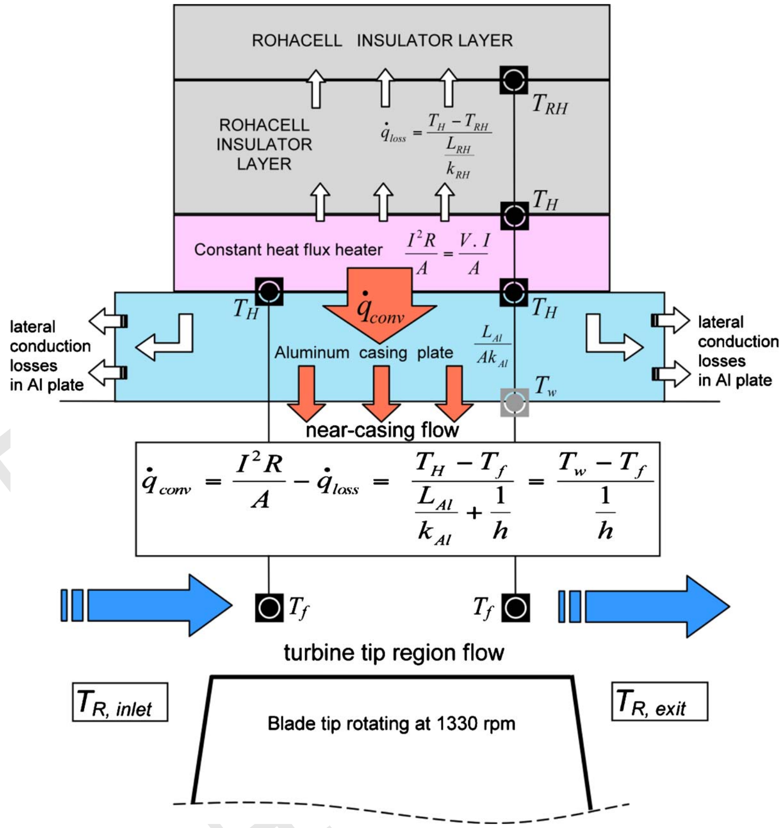

Fig. 5 Heat Transfer model for convective heat transfer coefficient measurements on the turbine casing surface (the model allows for lateral conduction losses)

The flat thermocouple junctions are 12 μm thick. There are two relatively thick layers of Rohacell insulating material flush mounted on top of the heater surface, as shown in Fig. 5. Table 3 includes all of the material thicknesses in the heat transfer composite surface and thermal conductivity values. Current multidimensional heat conduction analysis shows that the lateral conduction of thermal energy at the edges of the thin "heater surface" and low conductivity "Rohacell insulator" is extremely small and negligible. However, the heat conduction loss q_{loss} in Rohacell is not negligible in a direction normal to the heater,

$$q_{\text{loss}} = (T_H - T_{RH})/(L_{RH}/k_{RH}) \tag{1}$$

Due to extremely thin structure and the uniform internal heat generation by Joule heating in the volume of the heater, measured top and bottom surface temperatures T_H are very close to each other. The amount of heat flux conducted through the aluminum casing plate in a direction normal to the plate is

Table 3 Thermal conductivity and thickness values for the heat transfer surface components

Material	Thermal conductivity k (W/m K)	Thickness L (mm [in.])
Rohacell	0.030	4.064 [0.160]
Aluminum plate	202.4	0.762 [0.030]
Plastic layer	0.120	1.397 [0.055]
Heater (Minco)	0.981	0.500 [0.021]

$$q_{\text{conv}} = I^2R/A - q_{\text{loss}} = (T_H - T_f)/(L_{\text{Al}}/k_{\text{Al}} + 1/h) = (T_w - T_f)/(1/h) \tag{2}$$

Equation (2) shows the actual convective heat flux crossing the fluid-solid interface on the casing surface when the lateral conduction losses in Al plate are ignored. The heat loss to Rohacell layer is not negligible, as indicated by Eq. (1). Equation (2) also presents the convective heat transfer rate written between the heater T_H and the near-casing turbine fluid T_f. In this approach, a heat transfer coefficient h can be measured without measuring the wall temperature T_w directly. h is first calculated from Eq. (2) between T_H and T_f. This approach of measuring h by using the first part of Eq. (2) is highly practical and recommended because a direct measurement of wall temperature T_w is not necessary at the fluid-solid interface. A direct measurement of T_w may require a nonintrusive wall temperature measurement approach, which may be difficult to perform without any surface disturbances on the casing surface facing the tip gap region. The current strategy allows an indirect but accurate determination of T_w from Eq. (2) after h is obtained from the same equation. T_w can be calculated by rearranging Eq. (2) in terms of heater temperature T_H and freestream fluid temperature T_f,

$$T_w = T_H + h(T_H - T_f)(L_{\text{Al}}/k_{\text{Al}}) \tag{3}$$

A more accurate form of h can be obtained by quantifying lateral conduction losses in the aluminum plate. A three dimensional conduction heat transfer analysis including all complex geometrical features of the removable turbine casing is presented in the next few paragraphs. This computational effort reduces the measurement uncertainties in the measured convective heat transfer coef-

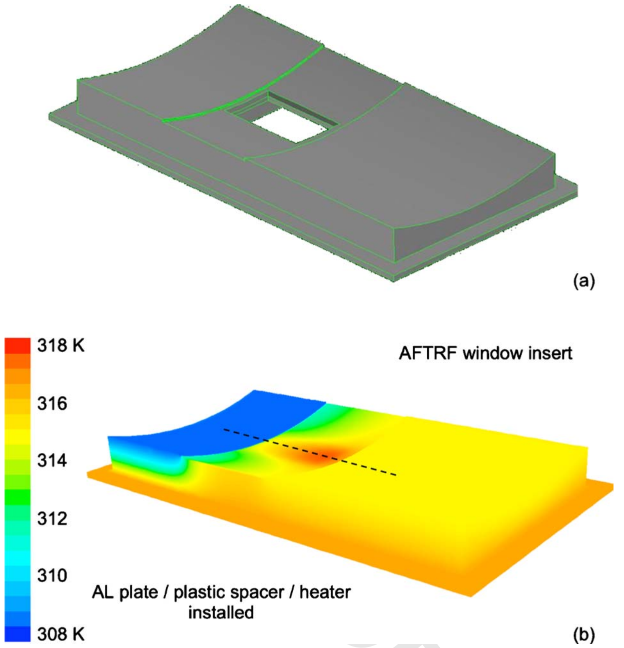

Fig. 6 3D solid model and conduction analysis results on removable turbine casing surfaces

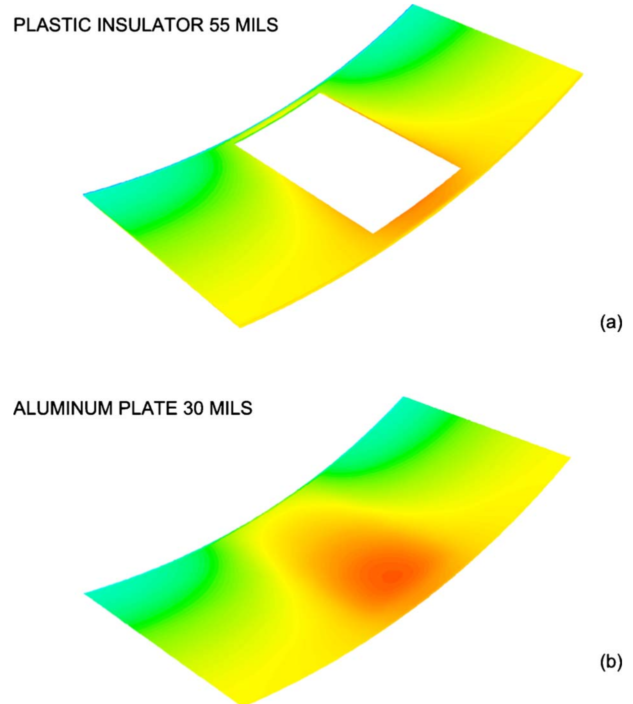

Fig. 7 Temperature distributions on the plastic spacer and aluminum casing plate (flow side)

ficient h. The correction is based on calculating the lateral conduction losses in the casing plate.

Lateral conduction losses in aluminum casing plate. Figure 6 presents the results from a 3D heat conduction analysis for the removable turbine casing. The removable turbine casing is an extremely thick precision machined aluminum with an average thickness of 50.8 mm (about 2 in.). The lateral heat conduction in the aluminum casing plate in this experiment was deduced from a 3D heat conduction analysis performed under realistic thermal boundary conditions. The steady-state thermal conduction equation $\nabla^2 T(x,y,z)=0$ was solved in the removable turbine casing with proper boundary conditions.

The constant heat flux heater shown in Fig. 5 is operated at a prescribed power I^2R value. Joule heating in the heater was simulated by distributing this I^2R value uniformly over the volume of the thin heater as an internal heat generation term. This is achieved by adding a source term to the energy equation in the numerical solution procedure.

Boundary conditions for conduction loss analysis. On the turbine flow side, the surface temperature upstream of the rotor leading edge is taken as the measured turbine rotor inlet temperature (or NGV exit temperature). The flow side surface temperature downstream of the rotor trailing edge is the same as the measured rotor exit temperature. The flush mounted aluminum casing plate has a convective type boundary condition on the flow side where a typical heat transfer coefficient h and a freestream reference temperature is specified at five axial positions. Measured ambient temperature outside the rig is specified on the external flat face of the removable turbine casing. All other boundaries on the side walls were taken as adiabatic. The heater surface area is about the same area as that of the small rectangular cut shown in Fig. 6(*a*).

Lateral conduction analysis results. The temperature distribution on the Al casing plate, as shown in Fig. 6, facing the rotating blade tips is characterized by the red zone on top of the heater area. Along the dashed line in the measurement area (in axial direction) the temperature distribution is reasonably uniform within 0.5 K. The minimum and maximum temperatures in Figs. 6 and 7 are 310 K (blue) and 317 K (red). All red hues are approximately corresponding to an area of 1 K temperature band.

Figure 7(*a*) shows the plastic spacer/insulator inserted between the removable turbine casing shown in Fig. 6(*a*) and the 0.030 in. thick aluminum plate. The heater is flush mounted on the convex side of the aluminum plate. Two layers of Rohacell insulator were located on top of the heater surface in order to reduce the heat losses to the ambient from the heater, as shown in Fig. 5. The low conductivity plastic spacer is essential in this measurement approach in reducing the heat losses in the 0.030 in. thick casing plate. Figure 8 presents the lateral conduction heat losses from the aluminum casing plate. $Q_{ABCD}=(Q_A+Q_B+Q_C+Q_D)$ is the sum of all thermal energy (W) laterally conducted from the rectangular area where the heater is flush mounted to the casing plate. Q_{RH} is the heat loss through the Rohacell insulator and Q_{HS} is the heat loss from the extremely narrow side faces of the heater volume with a thickness of 0.5 mm.

A new heat loss calculation was performed for each power setting using the 3D conduction analysis with proper boundary conditions. Figure 8 shows that the heat losses through the Rohacell layer and from the sides of the thin heater are extremely small when compared with the lateral conduction in the aluminum plate and the convective heat flux to the near-casing fluid in the turbine passage. A proper correction of convection heat flux term q_{conv} in Eq. (2) using lateral conduction losses is an important part in obtaining heat transfer coefficient on the turbine casing surface. Figure 9 presents the variation of convective heat flow over area A $[q_{\mathrm{conv}}\cdot A]$, lateral conduction loss Q_{ABCD} in aluminum casing plate, Rohacell layer losses, and heater side losses as a function of heater power setting I^2R. Rohacell layer heat losses and heater side losses are negligible when compared with the convective heat flux and lateral conduction loss.

Heat transfer coefficient from different power settings. The convective heat transfer coefficient is measured by using an arranged form of Eq. (2),

$$h=\frac{q_{\mathrm{conv}}k_{\mathrm{Al}}}{k_{\mathrm{Al}}(T_H-T_f)-L_{\mathrm{Al}}q_{\mathrm{conv}}} \tag{4}$$

where q_{conv} is obtained by subtracting the predicted heat loss q_{loss} from I^2R/A, as shown in Eq. (2). T_H is measured from a flush

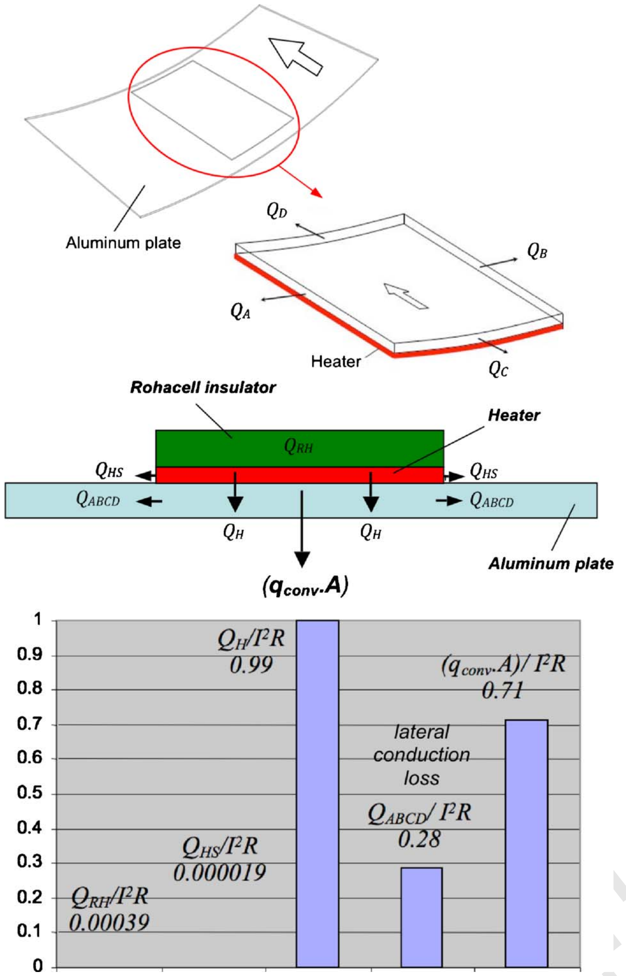

Fig. 8 Lateral conduction from the four sides of the area facing the heater and the final energy balance (I^2R=6.53 W)

mounted thermocouple embedded between the heater and the aluminum casing plate, as shown in Fig. 5. A nonintrusive and indirectly determined value of T_w is also available from Eq. (3).

The correct freestream reference temperature. Finding the most accurate value of the reference fluid temperature T_f in this problem is crucial. T_f is the reference freestream fluid temperature in the immediate vicinity of the casing surface facing the blade tips. Since this temperature in a turbine rotor monotonically decreases from rotor inlet to exit, a linear curve fit is obtained from the measured rotor inlet $T_{R,\mathrm{inlet}}$ and rotor exit $T_{R,\mathrm{exit}}$, as shown in Fig. 5. The two measurement thermocouples for $T_{R,\mathrm{inlet}}$ and $T_{R,\mathrm{exit}}$ are inserted into the freestream before and after the rotor. The junctions are in the turbine flow at a location about 25 mm away from the casing surface. The open circular symbols shown in Fig. 10 form an h measurement at axial location 1. A line fit passing from all circular symbols obtained from many different power settings is represented by $q_{\mathrm{conv}}=h\cdot(T_w-T_f)$ for the same turbine operating point. Maximum attention is paid to keep the corrected speed of the turbine facility and flow coefficient constant during the acquisition of all points at different heater power settings. The slope of this straight line is the convective heat transfer coefficient h.

The T_f value measured in the turbine freestream flow at this stage is not a proper reference temperature for this convective heat transfer problem. Since the thermocouples providing T_f are inserted well into the freestream (25 mm away from the casing), the measured local T_f are considerably different from the temperature of the fluid in the immediate vicinity of the casing. This observation is consistent with the data shown with circular symbols in

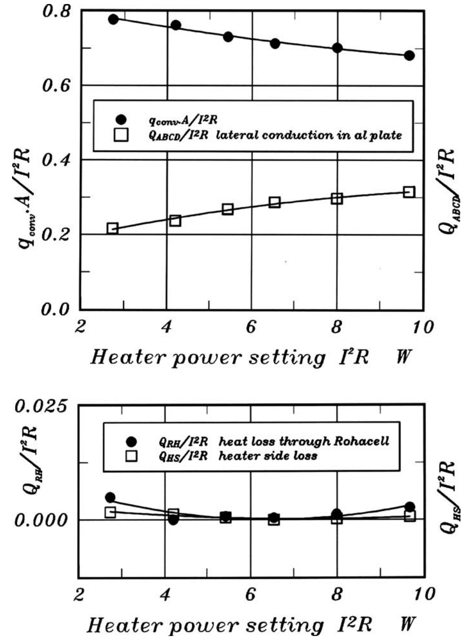

Fig. 9 Energy balance in the heat transfer surface in function of power setting

Fig. 10. The solid line connecting the circular symbols does not pass through the origin as $q_{\mathrm{conv}}=h\cdot(T_w-T_f)$ suggests. This is a clear indication of the fact that the initially measured T_f (defined by $T_{R,\mathrm{inlet}}$ and $T_{R,\mathrm{exit}}$) is not proper for the casing heat transfer problem. What happens when the solid line does not pass through is directly related to the observation made in Fig. 11. The computation of h at many different power settings at the same turbine flow condition does not yield to an invariant h. The open triangular symbols suggest that h varies strongly with increased heater power setting.

Direct measurement of T_{aw} as the correct freestream reference temperature. Using multiple heater power settings allows a simultaneous measurement of h and T_{aw}. h and $T_{aw}=T_f$ as two unknowns of $q_{\mathrm{conv}}=h\cdot(T_w-T_f)$ could be obtained from two independent measurement points obtained at two different power settings. Having many more points than two and using a first order line fit only reduce the experimental uncertainties in this process. The true reference temperature in this problem (adiabatic wall temperature T_{aw}) is obtained by shifting the original solid line to the left until it passes through the origin. The amount of this horizon-

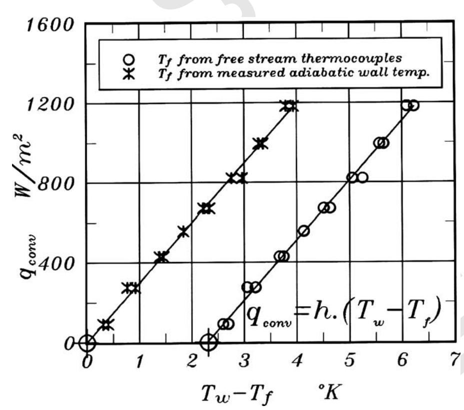

Fig. 10 Simultaneous determination of convective heat transfer coefficient h and freestream reference temperature from multiple heater power settings

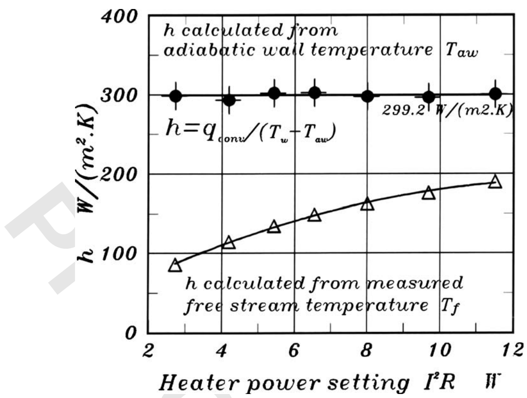

Fig. 11 Influence of proper freestream reference temperature on convective heat transfer coefficient

tal shift is the correction to be applied to initially suggested T_f. The corrected value of T_f is actually the same as the actual adiabatic wall temperature T_{aw}.

A validation of T_{aw} measurement. A useful check on the value of h obtained from the measured reference temperature T_{aw} is shown in Fig. 11. When h is calculated by using measured T_{aw} at many different power settings, a constant level of h is obtained, as shown by solid circular symbols. This constant level of h within experimental uncertainty indicates that the measured T_{aw} is the proper reference temperature for this convective heat transfer problem.

The procedure described in this section has the ability to measure the heat transfer coefficient h and freestream reference temperature $T_f=T_{aw}$ simultaneously in a nonintrusive way. A direct measurement of T_{aw} in the turbine in the tip gap region by an inserted probe is extremely difficult. Another complexity is that the reference temperature continually drops in the turbine due to the work extraction process gradually building up in the in the axial direction. Figure 11 is a good display of the fact that the measured heat transfer coefficient h (slope of the solid line in Fig. 10) is independently defined from the power setting and thermal boundary conditions $\Delta T=T_w-T_f$.

Axial distribution of h on the casing plate. Figure 12 presents heat transfer coefficient data at all five axial locations defined in Fig. 4. At this stage, q_{conv} is not corrected for lateral conduction losses yet. The same measurement methodology described in the previous paragraphs is applied at all five locations. A typical heat transfer experiment in AFTRF has an approximate duration of 50 min with h data obtained from eight to ten discrete heater power levels. No data are taken in the first 20 min to allow reasonably steady thermal and freestream conditions to develop in AFTRF.

Figure 13 shows the axial distribution of h at five axial locations on the casing plate facing the blade tips. The solid circles represent the data before a lateral conduction correction in the aluminum casing plate is applied. The magnitude of lateral conduction losses are carefully determined from a 3D heat conduction analysis described in Figs. 6–9. A proper heat loss analysis was performed for each power setting level carefully. A significant change in the overall magnitude of the heat transfer coefficients is observed after taking into account all energy losses from the Al casing plate, especially the lateral conduction losses. The casing plate measurement locations see the subsequent passage of tip leakage related fluid and passage fluid at blade passing frequency. The circumferential mixing in this near-casing area is inevitable. A proper lateral conduction calculation is essential to reduce the experimental uncertainties in this heat transfer measurement approach.

Experimental uncertainty estimates. The most significant goal of this study was to establish a steady-state casing heat transfer measurement system with reduced uncertainties. Since the number

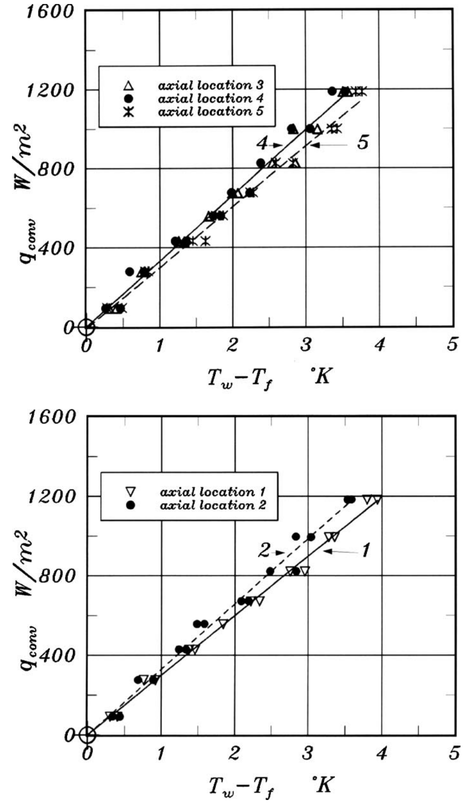

Fig. 12 Measured heat transfer coefficient *h* (slope) at five axial locations on the casing plate surface

of parameters to be controlled in the rotating rig is much larger than a typical wind tunnel study, a detailed uncertainty analysis is essential to control and reduce the experimental errors. The specific uncertainty approach follows the concepts developed by Kline and McClintock [15]. Our uncertainty analysis is based on our uncertainty estimates on reference freestream temperature, heater surface temperature, thermal conductivity, plate thickness, and aluminum casing lateral conduction error (Figs. 14 and 15).

Table 4 lists the magnitudes of all estimated basic measurement uncertainties. Uncertainty analysis showed that very low heater power levels typically less than 1 W have a tendency to increase $\delta h/h$. The lateral conduction loss could vary from 1% to 6% even after numerically correcting for the lateral heat conduction. This uncertainty is introduced to account for edge heat flux variations around a mean q_{conv} that already takes lateral conduction into

AQ: #4

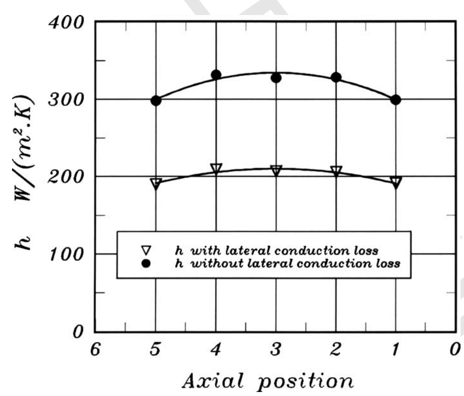

Fig. 13 Distribution of the heat transfer coefficient with respect to axial position on the casing surface

$$h = \frac{q_{conv}\, k_{Al}}{k_{Al}(T_H - T_f) - L_{Al}\, q_{conv}}$$

$$\delta h = \left[\left(\frac{\delta h}{\delta q}\delta q\right)^2 + \left(\frac{\delta h}{\delta k}\delta k\right)^2 + \left(\frac{\delta h}{\delta T_H}\delta T_H\right)^2 + \left(\frac{\delta h}{\delta T_f}\delta T_f\right)^2 + \left(\frac{\delta h}{\delta L}\delta L\right)^2\right]^{1/2}$$

$$\delta q = \delta q_{conv}$$

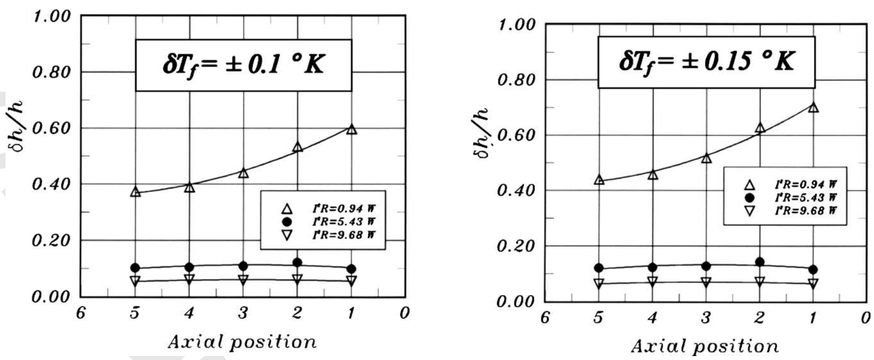

Fig. 14 Influence of reference temperature measurement error δT_f on $\delta h/h \delta q_{conv}/q_{conv} = \pm 0.01$, $\delta k = \pm 0.221$ W/m K, and $\delta L = \pm 25$ μm (0.001 mils)

account in a uniform way in axial direction. The uncertainty of heat transfer coefficient is estimated to be in a range from 5% to 8%.

3 Conclusions

A steady-state method for the measurement of convective heat transfer coefficient on the casing surface of an axial flow turbine is presented.

The current study presents a simultaneous measurement approach for both the heat transfer coefficient and the reference temperature of the near-casing fluid.

The nonintrusive determination of the reference near-casing fluid temperature $T_f = T_{aw}$ from the current method is highly effective in reducing the heat transfer measurement uncertainty.

The method developed is very suitable for research turbine applications where the freestream fluid continuously cools from rotor inlet to rotor exit due to work extraction.

Special attention is paid to the static casing region facing the rotor blades. The current T_{aw} measurement approach is a highly effective and nonintrusive approach for the fluid layers in the immediate vicinity of the static casing.

A significant improvement of the uncertainty of h is possible by taking lateral conduction losses in the casing plate into account. The lateral conduction losses resulting from each power setting of the "constant heat flux heater" were numerically evaluated on a high resolution 3D conduction grid prepared for the removable casing model.

The present method is able to take the variation of many turbine run time parameters into account during a 50 min run in which at least eight to ten heater power settings are used for the measurements.

A detailed uncertainty analysis is presented. The current heat transfer measurement method uncertainty is estimated to be between 5% and 8% of convective heat transfer coefficient h.

The heat transfer evaluation of many casing surface modifications and blade tip shape modifications are possible with the specific method presented in this paper.

Acknowledgment

The authors acknowledge the valuable comments and advice provided by Dr. R.E. Chupp of GE Power Systems throughout this study. They are indebted to Mr. Harry Houtz, Rick Auhl, Mark

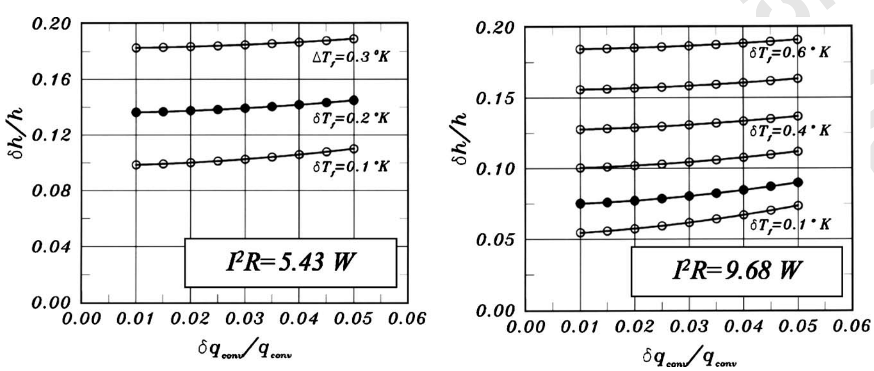

Fig. 15 Influence of heater power setting on $\delta h/h \delta T_H = \pm 0.15$ K, $\delta k = \pm 0.221$ W/m K, and $\delta L = \pm 25$ μm (0.001 mils)

Table 4 Uncertainty estimates

Quantity	Measurement error
T_f	$\delta T_f = \pm 0.15$ K
T_H	$\delta T_H = \pm 0.15$ K
k_{Al}	$\delta k_{Al} = \pm 0.221$ W/m K
L_{Al}	$\delta L_{Al} = \pm 0.001$ in. (25 μm)
q_{conv}	$\delta q_{conv}/q_{conv} = \pm 1-6\%$
h	$\delta h/h = \pm 5-8\%$

Catalano, and Kirk Hellen for their technical support. The authors also acknowledge the valuable support from the Department of Aerospace Engineering at Penn State University.

Nomenclature

A = heat transfer measurement area (m^2); also constant heat flux surface area
h = convective heat transfer coefficient (W/m^2 K)
h = also rotor blade height
I = dc level to heater
I^2R = Joule heating in the heater (W)
k = thermal conductivity
L = material thickness
N = rotational speed (rpm)
P_{o1} = stage inlet total pressure (Pa)
P_{o3} = stage exit total pressure (Pa)
P = turbine power output (kW)
Q_{RH} = total heat flow through Rohacell insulator (W)
Q_{HS} = heat loss from the sides of the 0.5 mm thin heater (W)
Q_H = $Q_H = (I^2R - Q_{RH} - Q_{HS})$ (W)
Q_{ABCD} = lateral conduction loss in al casing plate (W); all four sides, see Fig. 8
q_{conv} = convective wall heat flux (W/m^2)
q_{loss} = heat loss to ambient (through Rohacell) (W/m^2)
$q_{conv} \cdot A$ = convective heat flow through area A
$q_{conv} \cdot A$ = $(Q_H - Q_{ABCD})$ (W)
Q = turbine mass flow rate (kg/s)
r, R = radius
t = gap height between blade tip and outer casing
t/h = nondimensional average tip clearance t/h =0.76%
T_{o1} = stage inlet total temperature (K)
T_{o3} = stage exit total temperature (K)
T_{aw} = adiabatic wall temperature
T_f = freestream reference temperature (T_{aw})
$T_{R,inlet}$ = freestream total temperature at rotor inlet (measured 1.25 cm away from casing)
$T_{R,exit}$ = freestream total temperature at rotor exit (measured 1.25 cm away from casing)
U_m = rotor blade speed at midheight location
V = velocity
V = also dc voltage applied to the heater
q, x, r = tangential, axial, radial directions

Subscripts

aw = adiabatic wall
Al = Aluminum
f = freestream fluid reference
H = heater
RH = Rohacell insulator material
w = wall

References

[1] Butler, T. L., Sharma, O. P., Joslyn, H. T., and Dring, R. P., 1989, "Redistribution of an Inlet Temperature Distribution in an Axial Flow Turbine Stage," J. Propul. Power, **5**(1), pp. 64–71.
[2] Sharma, O. P., and Stetson, G. M., 1998, "Impact of Combustor Generated Temperature Distortions on Performance, Durability and Structural Integrity of Turbines," VKI Lecture Series 1998-02, Brussels, Belgium, Feb. 9–12.
[3] Harvey, N. W., 2004, "Turbine Blade Tip Design and Tip Clearance Treatment," von Karman Institute Lecture Series VKI-LS 2004-02, Brussels.
[4] Roback, R. J., and Dring, R. P., 1992, "Hot Streaks and Phantom Cooling in a Turbine Rotor Passage, Part-1 Separate Effects," ASME Paper No. 92-GT-75.
[5] Roback, R. J., and Dring, R. P., 1992, "Hot Streaks and Phantom Cooling in a Turbine Rotor Passage, Part-2 Combined Effects and Analytical Modelling," ASME Paper No. 92-GT-76.
[6] Takanishi, R. K., and Ni, R. H., 1990, "Unsteady Euler Analysis of the Redistribution of an Inlet Temperature Distortion in a Turbine," AIAA Paper No. 90-2262.
[7] Dorney, D. J., Davis, R. L., Edwards, D. E., and Madavan, N. K., 1990, "Unsteady Analysis of Hot Streak Migration in a Turbine Stage," AIAA Paper No. 90-2354.
[8] Dorney, D.J. and Schwab, R.J., 1995, "Unsteady Numerical Simulations of Radial Temperature Profile Redistribution in a Single Stage Turbine," ASME Paper No. 95-GT-178.
[9] Yoshino, S., 2002, "Heat Transfer in Rotating Turbine Experiments," D.Phil. thesis, Oxford University, New York.
[10] Thorpe, S. J., Yoshino, S., Ainsworth, R. W., and Harvey, N. W., 2005, "The Effect of Work Processes on the Casing Heat Transfer of a Transonic Turbine," ASME J. Turbomach., **128**, pp. 1–8.
[11] Thorpe, S. J., Yoshino, S., Ainsworth, R. W., and Harvey, N. W., 2004, "An Investigation of the Heat Transfer and Static Pressure on the Over-Tip Casing Wall of an Axial Turbine Operating at Engine Representative Flow Conditions: Part II, Time-Resolved Results," Int. J. Heat Fluid Flow, **25**(6), pp. 945–960.
[12] Rhee, D. and Cho, H.H., 2005, "Local Heat/Mass Transfer Characteristics on a Rotating Blade With Flat Tip in a Low Speed Annular Cascade: Part 2-Tip and Shroud," ASME Paper No. GT2005-68724.
[13] Camci, C., 2004, "Experimental and Computational Methodology for Turbine Tip De-Sensitization," VKI Lecture Series 2004-02, Turbine Blade Tip Design and Tip Clearance Treatment.
[14] Rao, M.N., Gumusel, B., Kavurmacioglu, L., and Camci, C., 2006, "Influence of Casing Roughness on the Aerodynamic Structure of Tip Vortices in an Axial Flow Turbine," ASME Paper No. GT 2006-91011.
[15] Kline, S. J., and McClintock, F. A., 1953, "Describing Uncertainties in Single-Sample Experiments," Mech. Eng. (Am. Soc. Mech. Eng.), **75**, pp. 3–11.

PROOF COPY [HT-10-1203] 025106JHR

AUTHOR QUERIES — 025106JHR

#1 AU: Please define HP if possible.
#2 Au: Please define NGV if possible.
#3 Au: Please reword sentences with color words as figures will only appear in black and white.
#4 Au: Figures must be cited in text. Please check our insertion of Figs. 14 and 15.